PRODUCTION OF LIME FROM LIMESTONE: PREDICTION OF LIME QUALITY AND CARBON-MONOXIDE LEVELS WITHIN A LIME KILN

P. Browne *

Workshop participants and other contributors:

P. Browne, A. Fitt [1], M. Jeoffreys [2],
S. Johnson [3], A. Lacey [4], T. Lange [5], H. Potgieter [6] and C. Thomas [7].

Abstract

We investigate lime kiln processes, namely the production of lime from limestone and the associated carbon-monoxide levels resulting from the heating process. Equations that govern lime production and carbon-monoxide levels are derived using first principles and data of carbon-monoxide levels are analyzed using wavelet analysis.

1 Introduction

The problems within the production of lime from limestone are worldwide phenomena. Much work has gone into the various aspects of the process

*School of Computational and Applied Mathematics, University of the Witwatersrand, Private Bag 3, Wits 2050, Johannesburg, South Africa. *e-mail: pbrowne@cam.wits.ac.za*

[1]School of Mathematics, University of Southampton, Southampton S017 1BJ UK. *e-mail: adf@maths.soton.ac.uk*

[2]School of Computational and Applied Mathematics, University of the Witwatersrand, Private Bag 3, Wits 2050, Johannesburg, South Africa. *e-mail: mjeoffreys@cam.wits.ac.za*

[3]*e-mail: sej@webmail.co.za*

[4]School of Mathematical and Computer Sciences, Heriot-Watt University, Riccarton, Edinburgh, EH14 4AS, UK. *e-mail: a.a.lacey@ma.hw.ac.uk*

[5]Optin, 9 Eldorado Road, Victory Park, Johannesburg, South Africa. *e-mail: tony@optin.co.za*

[6]School of Chemical and Metallurgical Engineering, University of the Witwatersrand, Private Bag 3, Wits 2050, *e-mail: hermanp@prme.wits.ac.za*

[7]*e-mail: cit@webmail.co.za*

(cf. Järvensivu *et. al.* [6], Meier *et. al.* [8] and McKenzie [7] for instance); however, the scope of this report is limited to the prediction of carbon-monoxide levels and lime quality within the lime kiln. Carbon-monoxide is a by-product of the burn process that needs to take place to convert the limestone into lime. Naturally we want to predict and control this to give a measure of the efficiency of burning. Due to the health hazard thereof we want accurate controls on the carbon-monoxide levels. Data are sent to a laboratory and are thus results that are 1 to 8 hours late. This is inadequate for the real-time environment of the problem. The measurements are inconsistent due to different people engaged in measuring, manual factors and varying methodologies. On line analyzers are inconsistent, fail, have drift and are costly to maintain. There is a need for a more consistent analyzer to replace the laboratory and the current analyzer.

This report is divided into three sections. In the section on First Principles, a system of equations that govern the lime production and the giving-off of carbon-monoxide is derived. In the second on Wavelet Analysis, the carbon-monoxide levels are examined using wavelets. In the final section conclusions and recommendations are given.

2 First principles

In order to have a better grasp of the problem, the problem must be defined in more specific terms. From there approximations can be made and something meaningful can be obtained.

2.1 Problem derivation

The limestone ($CaCO_3$) is fed into a vertical pre-heater at roughly room temperature of 30^oC. The stones have fairly consistent diameters of about 2cm-5cm. In the pre-heater the limestone is heated, by an air-stream leaving the kiln. The temperature of the limestone is 450^oC when entering the kiln. This heating of the limestone corresponds to a drop in the air-stream temperature from 1050^oC, as the air-stream leaves the kiln, down to 300^oC as air-stream leaves the pre-heater. The limestone then travels down through the 70 m kiln at a speed of $7/250$ $m.s^{-1}$, the kiln being tilted down at an angle of 3^o. At the same time, the kiln rotates with angular speed ω $rad.s^{-1}$ and causes the limestone to shuffle around in a motion similar to that of the angular rotation of the kiln. This results in the heating of the limestone being non-uniform through a cross-section. The limestone is heated by a flame extending 20 m from the lower end of the kiln, in which pulverized

coal is burnt. The coal is fed into the flame at a temperature of $600°C$. The burning leads to an air current flowing in the opposite direction to the limestone. At the entry point (for the limestone) of the kiln there are CO and O_2 gas sensors that measure the respective gas levels. After traversing down the kiln the lime (CaO) falls into a container which for the purposes of this project will not be in the model and can thus be ignored. Quality (meaning how well the limestone is converted to lime) measurements are taken hourly at the exit end of the kiln.

The problem is limited to one dimension, with the x axis running down the kiln decline. This can be done because variation across the kiln is neglected. Let $T_s(x)$ be the temperature of the solid (limestone); $T_g(x)$ be the temperature of the gas; $-u_g$ be the constant gas speed in the negative x direction; u be the constant limestone speed in the x direction; ρ, ρ_g be the limestone and gas densities respectively; $L(= 70m)$ be the length of the kiln; $L_f(= 50m)$ be where the flame ends. This allows the lime kiln process to be depicted as in Figure 1.

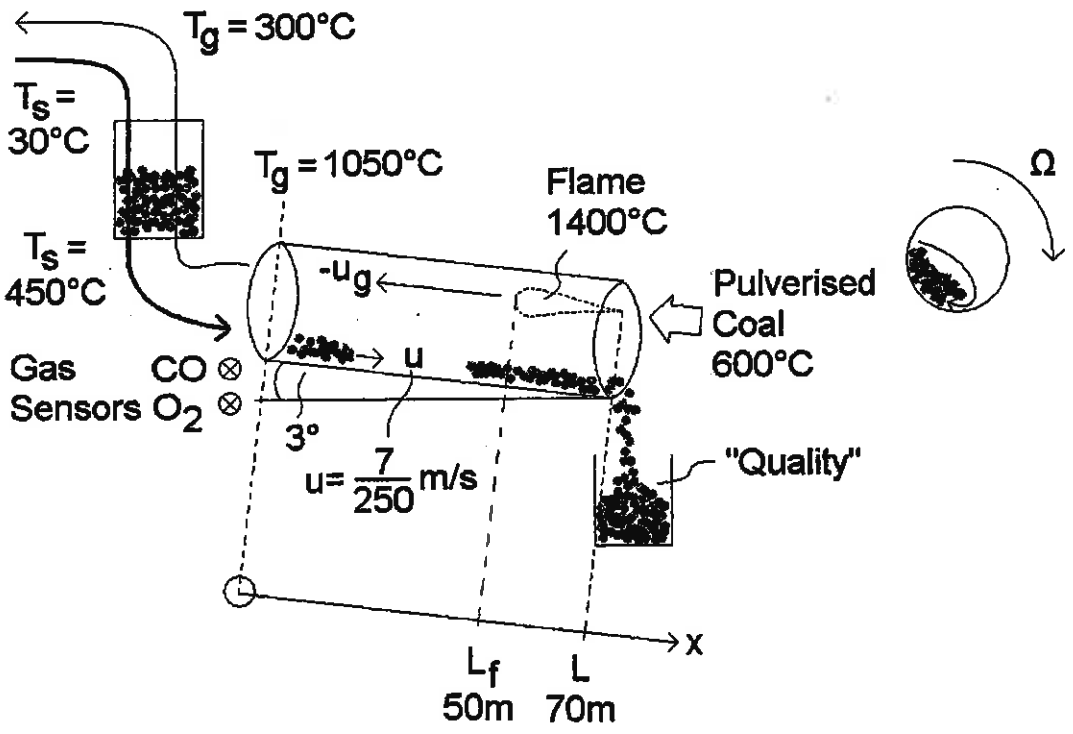

Figure 1: Lime kiln process

To analyze the main chemical reaction

$$CaCO_3 \rightarrow CaO + CO_2, \tag{1}$$

let $y(x)$ be the mass fraction of limestone ($CaCO_3$) in the solid; $c(x)$ be the mass fraction of lime (CaO) in the solid; and $z(x)$ be the amount of carbon dioxide (CO_2). For a meaningful model assume that the reactions are Arrhenius (see Holmsted and Williams [9] pages 707 - 709); the solids are well mixed due to tumbling and are uniformly heated; the stones themselves are in the region of $5cm$, yielding a diffusion time

$$T_D = \frac{l^2 \rho \, c_p}{k}, \tag{2}$$

of

$$T_D = \frac{(5 \times 10^{-3})^2 (2 \times 10^3)(10^3)}{0.5} \approx 100s. \tag{3}$$

Further, steady flow

$$\frac{D}{Dt} = \frac{\partial}{\partial t} + u \frac{\partial}{\partial x} = u \frac{\partial}{\partial x}, \tag{4}$$

exists for the limestone and, similarly (4) with $-u_g$ replacing u exists for the gas.

The change from limestone to lime is assumed to proceed at a rate proportional to the remaining amount of limestone with a temperature-dependent factor, so that

$$\frac{Dy}{Dt} = u \, y'(x) = -A \, y \, e^{-\frac{E}{RT_s(x)}}, \tag{5}$$

where E is the activation energy, R is the gas constant (measured in $J/mol \, {}^oK$) and $y(0) = y_0$. Also, A and E are known reaction constants. Due to conservation of mass, the amount of lime will be directly related to the amount of limestone from which it is converted, according to

$$c = \phi \, (y_0 - y), \tag{6}$$

where

$$\phi = \frac{[CaO]}{[CaCO_3]} = \frac{[20 + 16]}{[20 + 48 + 12]} = \frac{36}{80} \approx \frac{1}{2}. \tag{7}$$

From conservation of energy (heat) the rate-of-change of sensible heat (heat capacity x temperature) in the solid is given by the rate-of-production of heat by the conversion process (this is negative) plus the rate-of-heat-transfer from the gas:

$$Heat_{solid} = Heat_{reaction} + Heat_{transfer}, \tag{8}$$

and the rate-of-change of sensible heat in the gas is given by rate-of-production of heat by the combustion of the coal minus rate of heat transfer to the solid:

$$Heat_{gas} = Heat_{flame} - Heat_{transfer}. \tag{9}$$

The rate-of-increase of heat content of the solid in (8) is simply the rate-of-change of its temperature multiplied by the density and specific heat capacity c_p:

$$\rho\, c_p \frac{DT_s}{Dt} = u\, \rho\, c_p\, T_s'(x), \tag{10}$$

while the rate-of-absorption of heat by the reaction is the reaction-rate, as given in (5), multiplied by a heat-of-reaction, ψ (measured in $J.kg^{-1}$), to give

$$Heat_{reaction} = -A\, \psi\, y\, e^{-\frac{E}{RT_s(x)}}. \tag{11}$$

The heat-of-transfer will simply be the difference in temperatures between the solid and gas, multiplied by a heat-transfer constant h, hence equation (8) now becomes

$$u\, \rho\, c_p\, T_s'(x) = -A\, y\, \psi\, e^{-\frac{E}{RT_s(x)}} + h\, (T_g(x) - T_s(x)). \tag{12}$$

Similarly in (9),

$$Heat_{gas} = -u_g\, \rho_g\, c_{pg}\, T_g'(x). \tag{13}$$

However to simplify the model, assume that the flame heat is localized to the flame, hence

$$Heat_{flame} = KH(L_f - x), \tag{14}$$

where $H(L_f - x)$ is a Heaviside function and K is a heat constant. Equation (9) results in

$$-u_g\, \rho_g\, c_{pg}\, T_g'(x) = h\, (T_s(x) - T_g(x)) + KH(L_f - x). \tag{15}$$

Equations (5),(6),(12) and (15) form a basis for a system of equations which have initial conditions

$$y(0) = y_0\, kg, \quad c(0) = 0\, kg, \quad T_s(0) = T_{s0} = 450^oC, \quad T_g(0) = T_{g0} = 1050^oC. \tag{16}$$

A measure of Quality (Q) is

$$Q = \frac{c(L)}{\phi y_0}. \tag{17}$$

Also note that

$$\frac{\rho_g u_g}{\rho u} \approx 1. \tag{18}$$

In Figure 2 equations (5), (12) and (15) have been solved numerically using MATHEMATICA. The system was treated as an initial value problem and behaviour consistent with common logic is revealed. The limestone decays exponentially to zero as more and more of it is converted to lime, the limestone solid heats up to around 1400^oC of the flame, and the gas decreases from the flame temperature at $x = 70$ down to the temperature at $x = 0$. Also, the temperature differentials remains fairly constant along the flame. Considering (3) again, a diffusion time of $100s$ would require the limestone to travel $28m$ into the kiln at a speed of $\frac{7}{250} m.s^{-1}$. This is in harmony with Figure 2, seeing that the limestone has essentially all been converted to lime at the $30m$ mark.

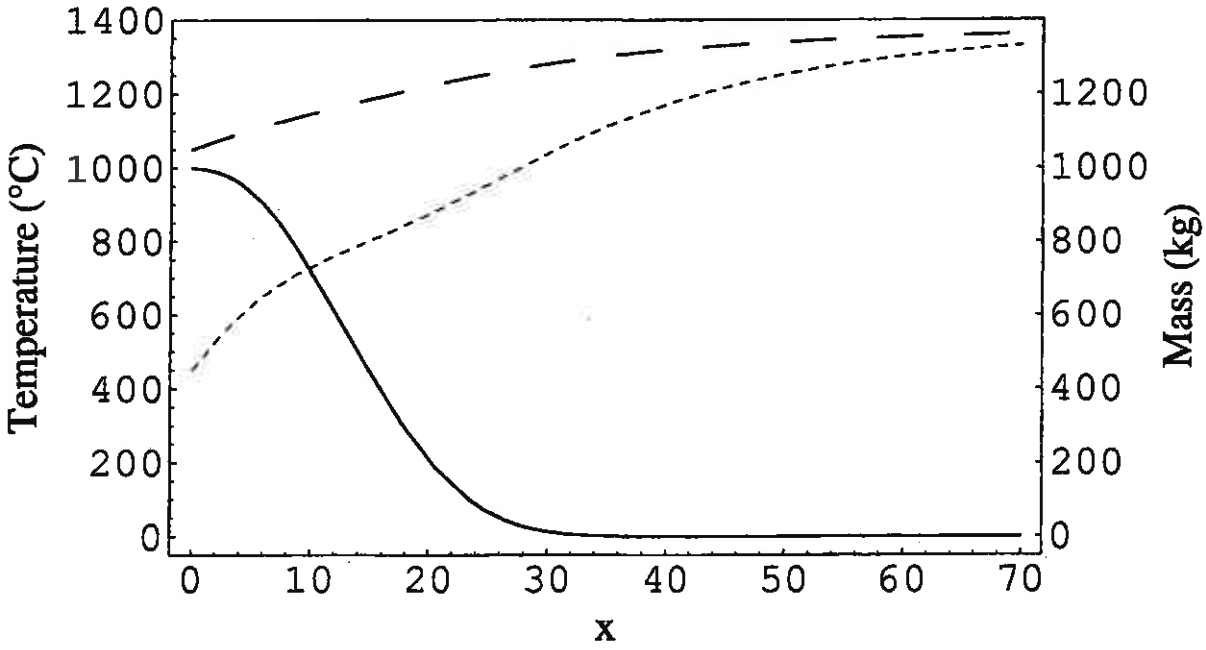

Figure 2: Plot of the amount of Limestone - y (___), in kg; the Temperature of the Solid - T_s (...) and the Temperature of the Gas - T_g (- -), both in ^oC; with $A = 0.5$, $h = 0.2$, $E = 10^5$, $R = 25$, u_g=100, $\psi = 25$, $c_p = 1$, $c_{pg} = 1000$, $K = 1$, $\rho = 100$, $\rho_g = 0.0001$, and $y_0 = 1000$.

2.2 Approximations

As we now have a more concrete basis to work from, the following approximations can be made

1. Large heat transfer constant (h)
2. High Activation Energy (HAE) Limit $\frac{E}{RT_{s0}} >> 1$.
3. Low Activation Energy (LAE) Limit $\frac{E}{RT_{s0}} << 1$.

2.2.1 Large heat transfer constant (h)

Large h implies that heat is transferred instantly from the gas to the solid and so $T_g(x) = T_s(x)$. Combine equations (12) and (15), and substitute (5), then by integrating one obtains

$$u\,\rho\,c_p\,T_s - u_g\,\rho_g\,c_{pg}\,T_s = A\,\psi\,u\,y + Kq(x), \tag{19}$$

where

$$q(x) = \int H(L_f - x)\,dx. \tag{20}$$

Now let

$$T_s(0) = T_g(0) = T_{s0}. \tag{21}$$

Applying initial conditions to (19), results in a solution of

$$u\,\rho\,c_p\,T_s - u_g\,\rho_g\,c_{pg}\,T_s = \psi\,u\,(y-y_0) + Kq(x) + (u\,\rho\,c_p - u_g\,\rho_g\,c_{pg})\,T_{s0}. \tag{22}$$

2.2.2 High activation energy (HAE) limit

For the HAE limit, the exponential term, $e^{-\frac{E}{RT_s(x)}}$, in equation (12) must be negligible, requiring the exponent to be sufficiently large. We examine the exponent at our initial condition

$$\frac{E}{RT_{s0}}, \tag{23}$$

with

$$E = 3.1\times10^{-6}\,J/kg = 3.1\times10^{-6}(40+12)\times10^{3}\,J/mol \;\approx\; 10^{5}\,J/mol, \tag{24}$$

which implies

$$\frac{E}{R} \approx 10^{4}K. \tag{25}$$

The temperature T_{s0} is of the magnitude of $10^3 K$, making the HAE limit

$$\frac{E}{RT_{s0}} \approx 10 > 1, \tag{26}$$

which in turn makes our exponential term in equation (12) negligible. The reaction now takes place over a small distance and the kiln is used to heat the particles. A system of equations

$$u\,\rho\,c_p\,T_s' = h\,(T_g - T_s) - \psi\,u\,\delta(x - x_R), \tag{27}$$
$$-u_g\,\rho_g\,c_g\,T_g' = h\,(T_s - T_g) + KH(L_f - x), \tag{28}$$

results, where δ is the Dirac-delta function, H is the Heaviside function, x_R is known from the heat balance equation and

$$y(x) = y_0\,H(x - x_R). \tag{29}$$

Equations (27) and (28) are linear and can be solved numerically or in closed form, that is, in terms of standard functions.

2.2.3 Low activation energy (LAE) limit

As an alternative, applying a LAE limit as well, would mean that we have a system of three equations

$$u_\rho\,c_\rho\,T_s' = h\,(T_g - T_s) - \psi\,A\,y, \tag{30}$$
$$-u_g\,\rho_g\,c_{pg}T_g' = h\,(T_s - T_g) + KH(L_f - x), \tag{31}$$
$$u\,y' = -A\,y\,. \tag{32}$$

Although this would lead to simplifications, these are not pursued here as (26) indicates that this limit is unlikely to be relevant.

2.3 Carbon-monoxide

For the modelling of the carbon-monoxide, three combustion equations

$$2C + O_2 \rightarrow 2CO + Heat, \tag{33}$$
$$2CO + O_2 \rightarrow 2CO_2 + Heat, \tag{34}$$
$$C + O_2 \rightarrow CO_2 + Heat, \tag{35}$$

are obtained. By the Law of Mass-Action (see pages 401 and 433 of Toon *et. al.* [10] for a more detailed explanation) the reaction rates in fluids

are proportional to concentrations to the power of the number of molecules involved. For example, the second reaction, (34), involves two carbon monoxide and one oxygen molecules, and its rate is therefore jointly proportional to the concentration of carbon monoxide, $[CO]$, squared and to the concentration of oxygen, $[O2]$. The first reaction involves carbon in a solid phase and can be expected to have a rate proportional to the solid surface area, that is, proportional to the linear dimension of the particles squared. With concentration proportional to volume occupied by the particles, that is, to the linear dimension cubed, we get a factor $[C]^{2/3}$. This is multiplied by a factor $[O2]$ due to the first-order involvement of the oxygen in the gas phase. All the reaction rates will depend upon concentration, so a usual Arrhenius factor [9], of the form $e^{-\frac{E}{RT}}$, is also included:

$$R_1 = [O_2][C]^{\frac{2}{3}} A_1 \, e^{-\frac{E_1}{RT_g}}, \tag{36}$$

$$R_2 = [CO]^2[O_2] A_2 \, e^{-\frac{E_2}{RT_g}}, \tag{37}$$

$$R_3 = [O_2][C]^{\frac{2}{3}} A_3 \, e^{-\frac{E_3}{RT_g}}. \tag{38}$$

The Heat of Burning will now be

$$H_B = \psi_1 R_1 + \psi_2 R_2 + \psi_3 R_3, \tag{39}$$

where the ψ_i's are stoichiometric coefficients (cf. [10] and [9]). At this point note that E_2 is known in the literature, but that there is uncertainty around E_1 and E_3, and that A_1, A_2, A_3 are unknown.

This then leaves four differential equations

$$-u_g[O_2]' = -(R_1 + R_2 + R_3), \tag{40}$$

$$-u_g[CO]' = \phi_1 R_1 - \phi_2 R_2, \tag{41}$$

$$-u_g[C]' = -(\phi_1 - 1)R_1 - \phi_3 R_3, \tag{42}$$

$$-u_g \, c_{pg} \, \rho_g \, T_g' = h \, (T_s - T_g) + H_B, \tag{43}$$

to which the equations for T_s and y are coupled. This results in a 6x6 nonlinear system of ordinary differential equations which could be solved numerically, but without values for the respective constants.

3 Wavelet analysis

Due to the nature of the data, Fourier Analysis is not beneficial. In this type of analysis, the Fourier transform is a function of frequency and amplitude. Thus the underlying data needs to have some form of recognizable pattern. The power of Wavelet Analysis lies in the fact that even if there seems to be no visible pattern, it will reduce noise to a level where an underlying pattern emerges. The Wavelet transform is rather a function of scale and position and not frequency and amplitude, as with Fourier Analysis. Base wavelet types have been studied and chosen to reveal the underlying pattern of the data for different types of data. Within these types there are different variations. Some of the most common types are Daubechies [2], Haar [4] and Biorthogonal [1] wavelets. After choosing a base wavelet, the methodology used to perform the Wavelet transformation is standard, in that a small-scale filter filters-out the data that have smaller scale repetition, to reveal a reduced data set that has a larger scale. The process is repeated iteratively, on each new reduced data set, until an underlying pattern can be seen that has a large scale. After examining different wavelet bases on the carbon-monoxide levels, the one that produced the most observable patterns was that of the Daubechies (db) wavelets.

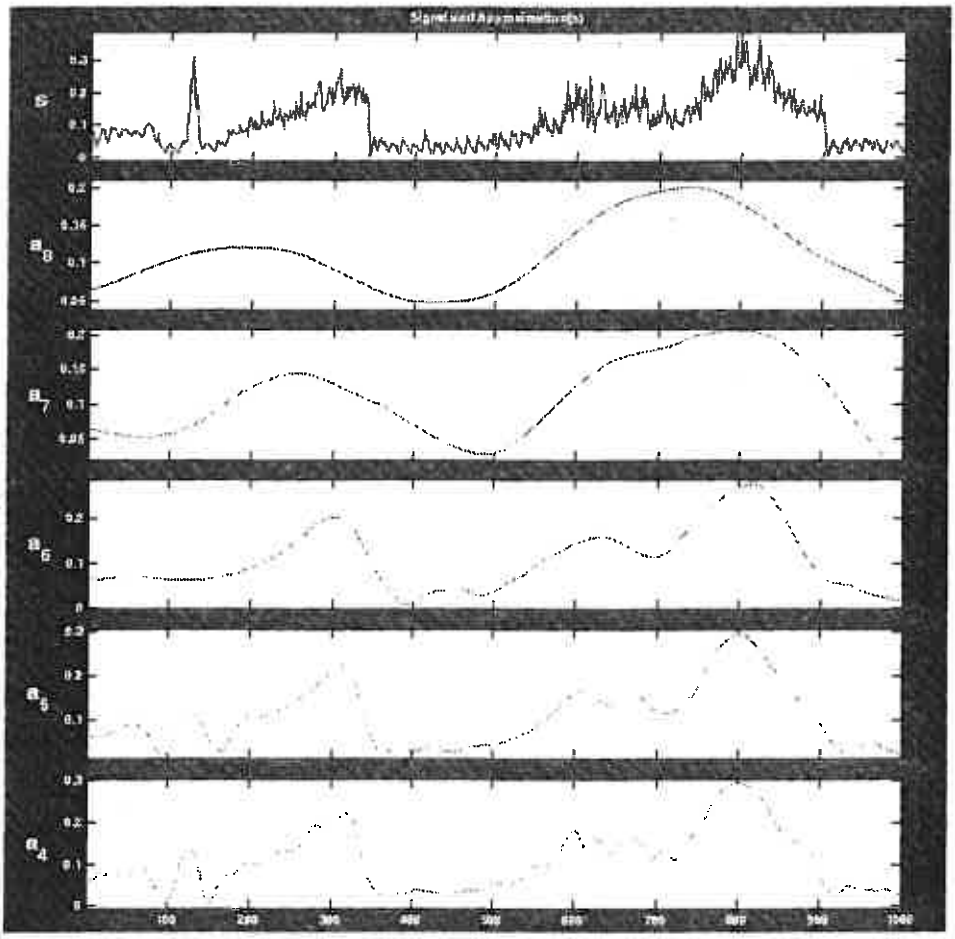

Figure 3: 1000 CO Level Data Points at 15 second intervals, db6 wavelet

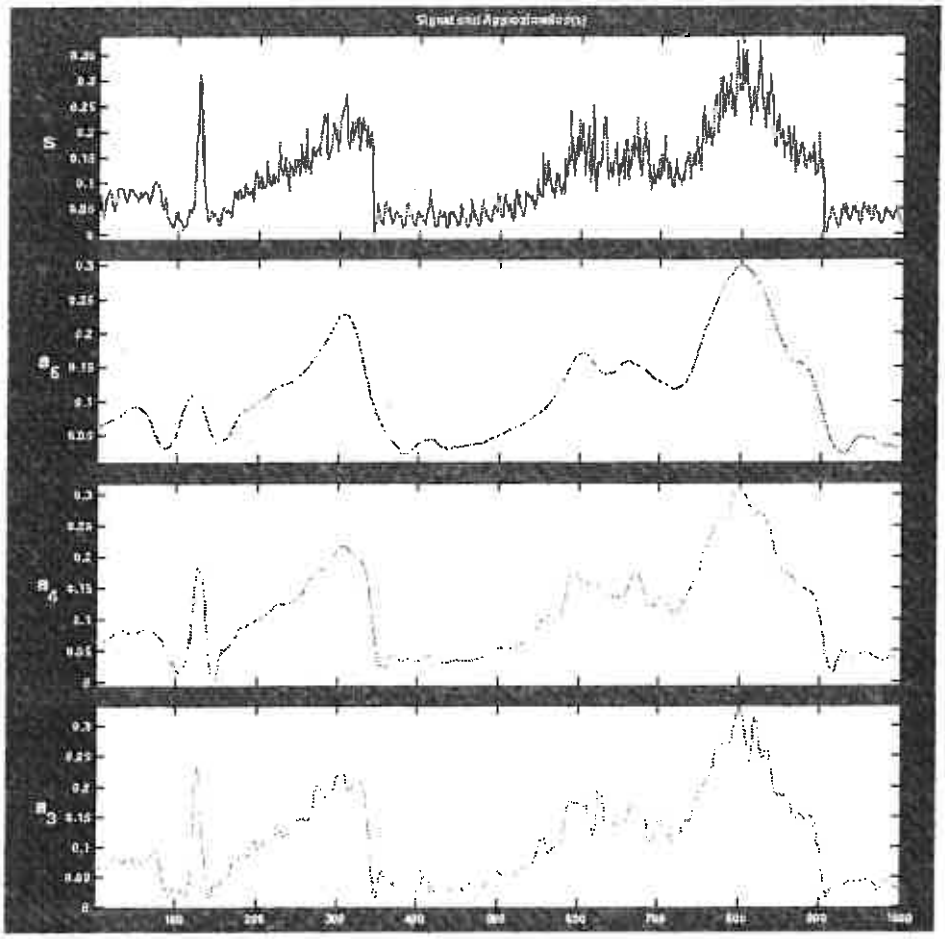

Figure 4: 1000 CO Level Data Points at 15 second intervals, db5 wavelet

As can be seen in Figure 3 and Figure 4, patterns emerge for Daubechies' db6 and db5 wavelets respectively, which could be useful for prediction purposes. Due to limitations on time, data were only considered for 1000 points at a 15 second interval, which is 250min or approximately 4 hours. It would be of great interest to extend this to have more data points to see if the same pattern continues. In these figures, s is the original signal, and a_i is the reduced data set, that has been reduced i times.

In Figure 5, the carbon-monoxide level is examined for 46893 points at 15 second intervals or approximately 11723 minutes or 195 hours and where the Daubechies' db2 wavelet was repeated until level 5. The data are perhaps too large to see any patterns, however it can already be seen that the reduced data set seems to be more predictable now that the data of smaller scale has been removed. The gap in the figure is as a result of the wavelet analysis itself. Because repetitions to such high levels have taken place, it means that where the data are not as highly small-scaled as in other areas, it falls away.

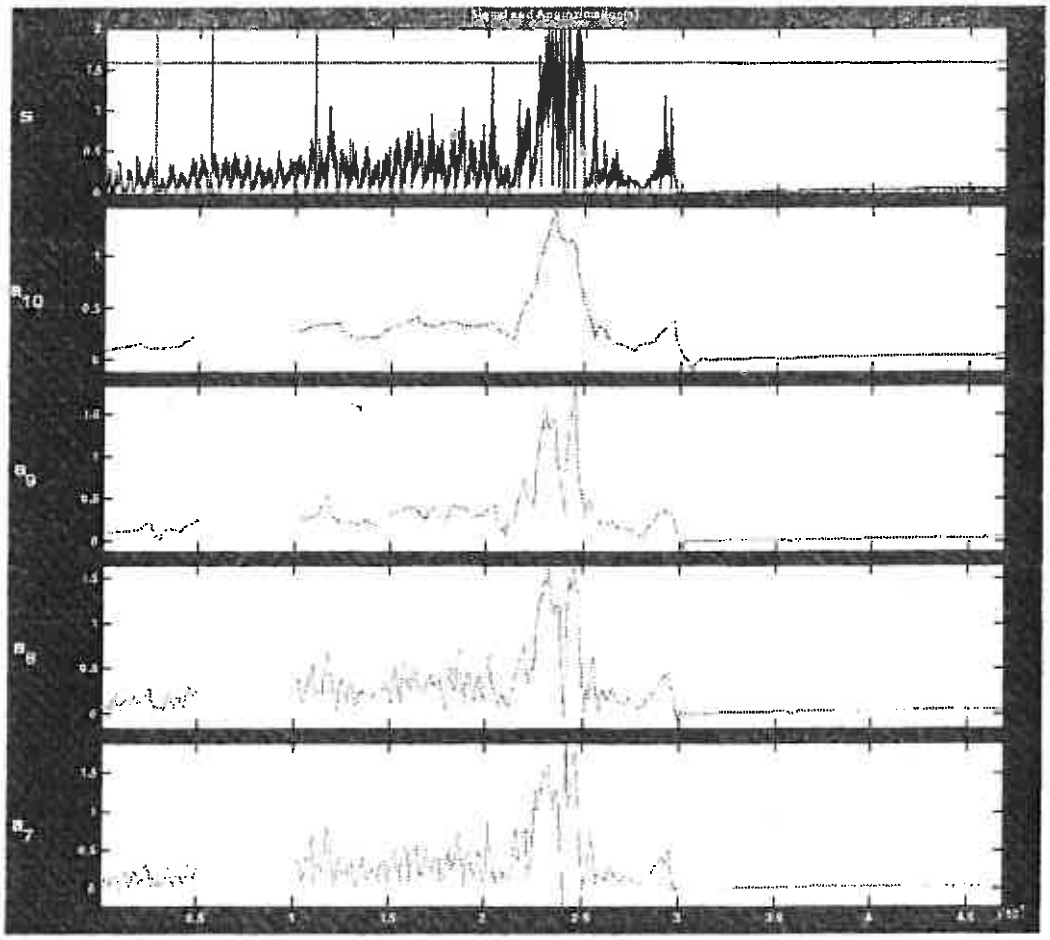

Figure 5: 46893 CO Level Data Points at 15 second intervals, db2 wavelet

4 Conclusions

This particular problem of modelling the production of lime from limestone has produced acceptable results in the sense that, when we examine Figure 2, we are able to see that our graph begins to mirror common sense and the real world situation. However more work would be required to examine the numerics of the equations derived from first principles, and to begin incorporating other assumptions into the derivation. Also, by sourcing the parameter values used from pre-existing literature, we would be able to introduce non-dimensional variables to write the equations in dimensionless form. The dimensionless numbers would allow for easier analysis of the equations, with the magnitudes allowing further insight into approximate analytical solutions as well numerical solutions. The wavelet analysis revealed that there is further scope for investigation that can take place by extending the current wavelet analysis that we have done. The extension

should include the data for other parameters of the problem, a shorter time interval and a greater window of analysis.

References

[1] Cohen, A., Daubechies, I. and Feauveau, J. Biorthogonal bases of compactly supported wavelets, *Comm. Pure Appl. Math.* **45** (1992), 485-560.

[2] Daubechies, I. Orthogonal bases of compactly supported wavelets, *Comm. Pure Appl. Math.* **41** (1988), 909-996.

[3] Daubechies, I. Ten Lectures on Wavelets, Capital City Press (1992).

[4] Haar, A. Zur theorie der orthogonalen Funktionsysteme, *Math. Annal.* **69** (1910), 331-371.

[5] Holschneider, M. Wavelets. An Analysis Tool, Oxford University Press (1995).

[6] Järvensivu, M., Juuso, E. and Ahava, O. Intelligent control of a rotary kiln fired with producer gas generated from biomass, *Engineering Applications of Artificial Intelligence* **14** (2001), 629-653.

[7] McKenzie, L. The Microscope: A Method and Tool to Study Lime Burning and Lime Quality, Proceedings of the Seventeenth Annual International Conference On Cement Microscopy (1995).

[8] Meier, A., Gremaud, N. and Steinfeld, A. Economic evaluation of the industrial solar production of lime, *Energy Conversion and Management* **46** (2005), 905-926.

[9] Olmsted, J. and Williams, G. Chemistry: The Molecular Science. Wm. C. Brown Publishers (1994 and 1997).

[10] Toon, E., Ellis, G. and Brodkin, J. Foundations of Chemistry, Holt, Rinehart and Winston (1968).